DOI 10.1007/s11106-015-9644-4
Powder Metallurgy and Metal Ceramics, Vol. 53, Nos. 9-10, January, 2015 (Russian Original Vol. 53, Nos. 9-10, Sept.-Oct., 2014)

EFFECT OF THE PARAMETERS OF MELT DISPERSION PROCESS ON THE MORPHOLOGY, STRUCTURE, AND PARTICLE SIZE OF WATER-ATOMIZED ALUMINUM POWDERS

O. D. Neikov,[1,2] G. I. Vasil'eva,[1] A. V. Samelyuk,[1] V. G. Tokhtuev,[1] V. A. Zhoga,[1] E. A. Potipaka,[1] and I. I. Odokienko[1]

UDC 621.762

Water atomized powders of aluminum and aluminum alloys produced at a melt temperature of 690–1350°C and a water pressure of 2.0–16.0 MPa are studied. It is established that the melt temperature and the water pressure in these ranges hardly affect the shape of particles similar in size and their surface geometry. The particle size is a key parameter in the shaping and structure formation of particles. The heat transfer process occurs in film boiling conditions because of high temperature difference at 380–935°C and heat flux much higher than critical. It is established that the heat transfer coefficient at a water pressure of 10–14 MPa changes from 10^4 to $4 \cdot 10^4$ W/(m$^2 \cdot$ °C) with a standard deviation of ±5.5% as the heat flux changes from 10^7 to $5 \cdot 10^7$ W/m^2. This technique to determine the heat transfer coefficient involves the calculation of the cooling rate using the dendritic parameter, which allows increasing the accuracy of calculation.

Keywords: *dispersion, melt, water pressure, heat exchange, cooling rate, film boiling, shaping of particles, particle size composition.*

INTRODUCTION

Morphology, structure, and size distribution of powder particles are important for manufacturing products with desired properties by powder metallurgy methods. Despite the theoretical justification of melt dispersion [1–4], computational methods to determine the technological parameters governing the production of powders with specified particle shape and size have scarcely been developed because it is difficult to analytically describe the hydrodynamic and heat exchange processes accompanying the interaction between high-pressure water jet and molten metal. Therefore, experimental research needed to establish the dependence of powder characteristics on the most important process parameters (such as the water jet speed and melt temperature) remains relevant [5, 6]. Studies on metal spraying with high-pressure water are not as numerous as those on metal dispersion by high-pressure gas jets. This applies especially to aluminum and aluminum alloys: their high reactivity leads to the oxidation of powders and evolution of hydrogen.

The purpose of this study is to investigate the dependence of surface morphology, particle structure, and particle size of powders on the pressure of water as an energy carrier and the temperature of the molten metal over a wide range of these parameters, and to compare the results with calculations.

[1]Frantsevich Institute for Problems of Materials Science, National Academy of Sciences of Ukraine, Kiev, Ukraine.

[2]To whom correspondence should be addressed; e-mail: neiko@mail.ru.

Translated from Poroshkovaya Metallurgiya, Vol. 53, No. 9–10 (499), pp. 13–23, 2014. Original article submitted August 14, 2013.

MATERIALS AND METHODS

Standard aluminum 99.7 wt.% Al (ISO 209-1) was selected as a model alloy to avoid the difficulties associated with finding the physical properties (required to calculate the characteristics of powders) of an aluminum melt of complex composition. Also, zirconium doped alloys of the system Al–5 wt.% Mg were investigated. The object of study was water atomized powders produced at a metal temperature of 690–1350°C and a water pressure of 2.0–16.0 MPa.

The powders were produced using a pilot plant [7] and following a procedure developed at the Institute for Problems in Materials Science, National Academy of Sciences of Ukraine (IPMS). The melt was drained from a crucible through a 7 mm hole in its bottom. The injector was equipped with eight nozzles, located on its circumference. They focus high-pressure water jets into a point at which they hit at an angle of 17° the melt flowing under gravity.

The size distribution of dried powder particles was determined by dry sieving, according to ISO 4497. The classification of the powder was improved by sieving small portions (150−200 g) of the powder through a testing screen. Upon sieving, the screen was subject to ultrasonic cleaning in an alkaline solution.

For structural studies, powder samples compacted into tablets with a porosity of 25% were electropolished in a mixture of $HClO_4$ (70 mL) and CH_3COOH (930 mL). The structural studies were performed using a scanning electron microscope (SEM).

The cooling rate of powders was calculated from the dendritic parameter [8], which was determined from the average distance between second-order dendrite branches if the structure is dendritic and from the average grain size if the structure is non-dendritic. The following equation was used:

$$v = a/l^n, \tag{1}$$

where v is the cooling rate, K/sec; l is the distance between second-order dendrites or the non-dendritic grain size, μm; a and n are constants.

For aluminum alloys we have $a = 100$, according to [9]. The value of n depends on the grain shape and varies between 0.25 and 0.5. For example, $n = 1/3$ for equiaxed grains. The grain size was determined from micrographs.

Since the size distribution of water-atomized powder particles is logarithmically normal [7, 10], the median diameter was determined from the distribution plotted on a logarithmic probability graphing paper.

The determining parameter in predicting the particle shape [1] is the ratio of spheroidizing time τ_{sph} to cooling time τ_{cool}:

$$\varepsilon = \tau_{sph} / \tau_{cool}. \tag{2}$$

The time of cooling of a melt drop to the liquidus temperature was calculated by the following formula [1]:

$$\tau_{cool} = d_d \frac{c_m \rho_m}{6\alpha} \ln \frac{t_m - t_w}{t_{liq} - t_w}, \tag{3}$$

where d_d is the drop diameter; c_m is the heat capacity of the melt; ρ_m is the density of the melt; α is the heat transfer coefficient; t_m is the initial temperature of the melt; t_{liq} and t_w are the liquidus temperatures of the drop and the water (where it contacts with the drop), respectively.

The spheroidizing time of a drop was calculated by the following formula [1]:

$$\tau_{sph} = \frac{3\pi^2 \mu}{4V\gamma_m} \left(r_{st}^4 - r_d^4 \right), \tag{4}$$

where μ is the dynamic viscosity of the melt; V is the volume of the drop; γ_m is the surface tension of the melt; r_{st} and r_d are the radius of the melt strand and the drop, respectively.

The radius of the melt strand was calculated by the formula given in [5] with reference to [11]:

$$r_{st} = 0.82 d_d^{1.09} \gamma_m^{0.09} \nu_m^{-0.18} \rho_m^{-0.09}, \quad (5)$$

where ν_m is the kinematic viscosity of the melt.

The main difficulty in the calculation of the cooling rate is to determine the heat transfer coefficient. Heat exchange during cooling of the melt drop is determined by boiling heat transfer. This process is very complex and is largely chaotic, even with stable heat supply in stationary conditions [12]. No analytical description of the process has been given yet; therefore, the crucial role belongs to experiments and similarity theory with dimensional analysis.

During dispersion of the melt by high-pressure water jets, the heat exchange is complicated by the rapid cooling of the drop and the time-dependent heat flux. In such circumstances (unsteady heat exchange), only the average heat transfer coefficient can be used at all stages of drop cooling.

Empirical formulas to determine the heat transfer coefficient in different boiling conditions are presented in [12, 13]. However, they apply to boiling on plates and cylindrical surfaces at atmospheric pressure in steady heat exchange conditions, which are very different from the heat exchange conditions during dispersion of a melt by high-pressure water.

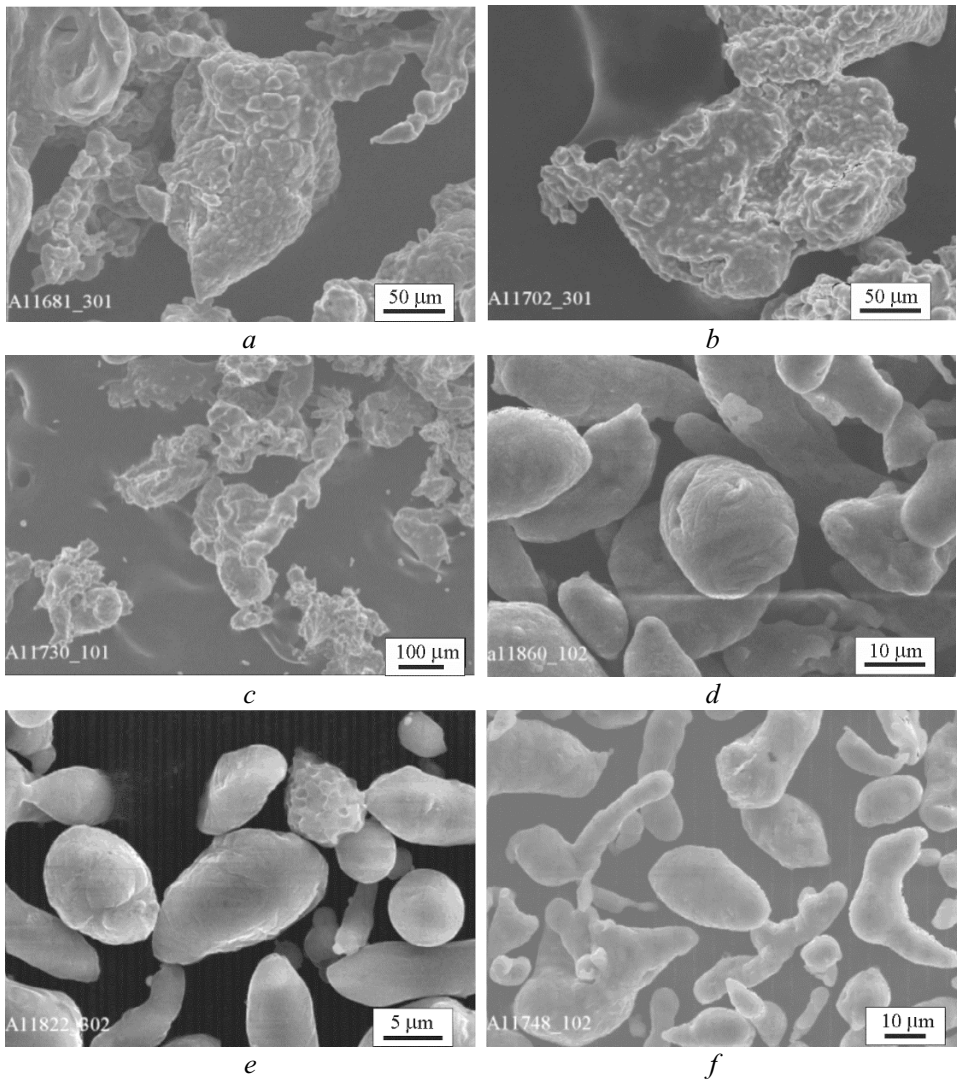

a *b* *c* *d* *e* *f*

Fig. 1. Typical configuration and morphology of particles similar in size (>50 μm (*a–c*) and <20 μm (*d–f*)), produced at a melt temperature of 1000°C and different water pressures: 3 (*a*), 10 (*b*), 16 (*c*), 2.0 (*d*), 6.2 (*e*), and 10 MPa (*f*)

The most reliable data on the cooling rate can be obtained by the method from [7] using data on the structure of the melt in particles solidified after atomization. Then, the average heat transfer coefficient of the drop can be calculated using Eq. (3).

We propose to use this method to determine the heat transfer coefficient of drops of different size under different conditions (variable water pressure and temperature of the melt).

RESULTS OF RESEARCH

Morphology of Powders. Figure 1 shows micrographs of the water atomized powders produced by dispersing the melt at 1000°C in the pressure range 2.0–14 MPa. It is characteristic that the pressure of the water hardly affects the shape and the surface geometry of either particles larger than 50 μm (Figs. 1*a–c*) when $\tau_{sph} > \tau_{cool}$ or fine particles (Figs. 1*d–f*) when the spheroidizing time is either shorter or equal to the cooling time.

Also, the temperature of the melt at temperature 690–1000°C and a water pressure of 10–14 MPa does not affect the shape and surface geometry of particles similar in size (Fig. 2).

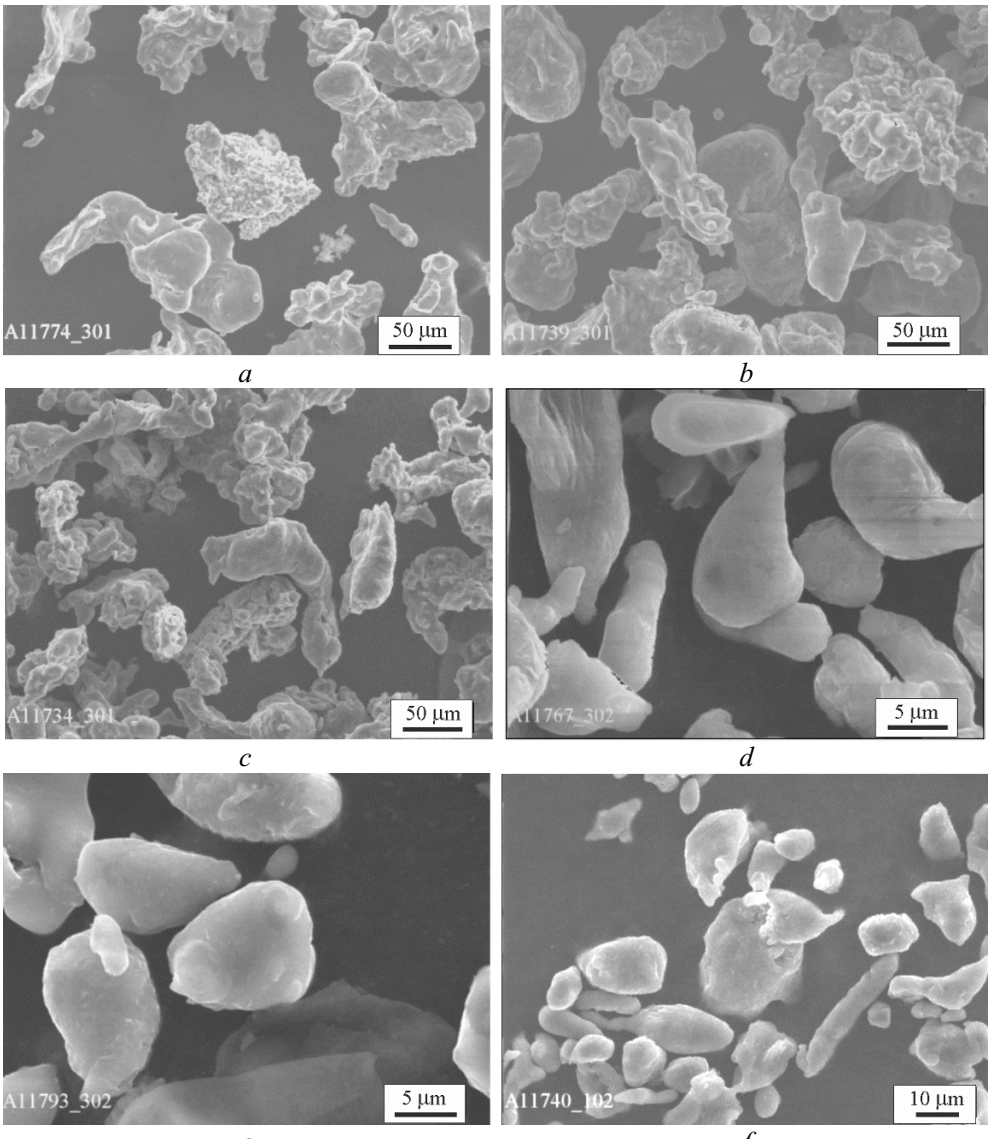

a *b* *c* *d* *e* *f*

Fig. 2. Typical configuration and morphology of particles similar in size (>50 μm (*a*–c) and <20 μm (*d–f*)), produced at water pressures 10−14 MPa and at melt temperatures of 690 (*a*), 900 (*b*), 1000 (*c*), 690 (*d*), 800 (*e*), and 1000°C (*f*)

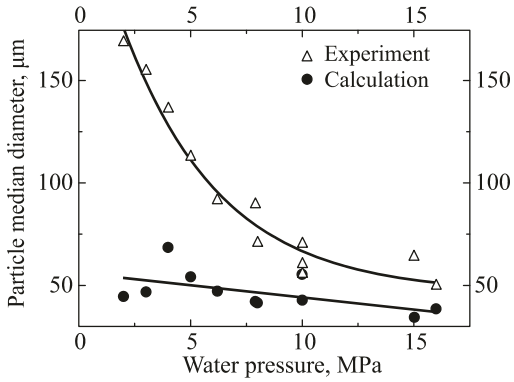

Fig. 3. Variation of the powder median diameter with the water pressure at a melt temperature of 1000°C

Particles larger than 50 μm have an awkward shape and surface geometry with irregularities particles. The larger the particles, the more there are such irregularities. Particles smaller than 20–30 μm become smoother with further decrease in size, spheroidizing completing in particles 7–5 μm in size. Thus, the particle size is the main factor affecting the particle shape regardless of the water pressure (2.0–14 MPa) and the melt temperature (690–1000°C). However, the particle size composition of the powder is strongly dependent on pressure and temperature on.

Particle Size Composition. Figure 3 shows the variation of the powder median diameter with the water pressure (2.0–16 MPa) at a melt temperature of 1000°C.

The experimental data were fitted by the following equation:

$$d_{50} = 45.9 + 205\exp(-p/4.38), \tag{6}$$

and the calculated values were fitted using the following formula in [14]:

$$d_{50} = 55.9 - 1.175p, \tag{7}$$

where p is the pressure of the water.

The median diameter was calculated by the formula

$$d_{50} = 4.97\frac{G_m^{1.24}}{G_w^{0.3}}\frac{\nu_m^{0.5}}{\gamma_m^{0.15}D_j^{1.03}\rho_m^{0.56}\nu_w^{0.07}V_w^{0.96}(\sin\beta)^{0.96}\rho_w^{0.25}}, \tag{8}$$

where G_m and G_w are the mass flow rates of the melt and water, respectively, kg/sec; V_w is the speed of water jet, m/sec; ρ_m and ρ_w are the densities of the melt and water, respectively, kg/m^3; γ_m is the surface tension coefficient of the melt, N/m; D_j is the melt jet diameter, m; ν_w is the kinematic viscosity of water, m^2/sec; β is the attack angle of the water jets. To calculate the median diameter, the following parameters were used: G_m = 0.042–0.1 kg/sec, G_w = 1.33–3.1 kg/sec, $\nu_m = 7.52 \cdot 10^{-7}$–$12.3 \cdot 10^{-7}$ m^2/sec, V_w = 97–137 m/sec, ρ_m = 2235–2357 kg/m^3, $\nu_w = 1.4 \times \times 10^{-6}$ m^2/sec.

The calculated values of the median diameter are close to the actual values at 12–16 MPa (Fig. 3). The difference increases with decreasing pressure: the actual values of the particle size are greater than the calculated values by a factor of more than 3 when p = 2.0 MPa. Such a disagreement between the calculated and actual values can be explained by the fact that the semi-empirical formula (8) has been derived using similarity theory and dimensional analysis for water-dispersion of alloyed steels [14].

The size distribution of powder particles of aluminum alloys is logarithmically normal [7, 10] and, thus, is characterized by two parameters: the average median diameter d_{50} of particles and standard (root-mean-square) deviation σ,

$$\sigma = \frac{d_{84.1}}{d_{50}} = \frac{d_{50}}{d_{15.9}}, \tag{9}$$

where $d_{84.1}$ and $d_{15.9}$ are the diameters corresponding to 84.1 and 15.9 wt.% of powder particles [15].

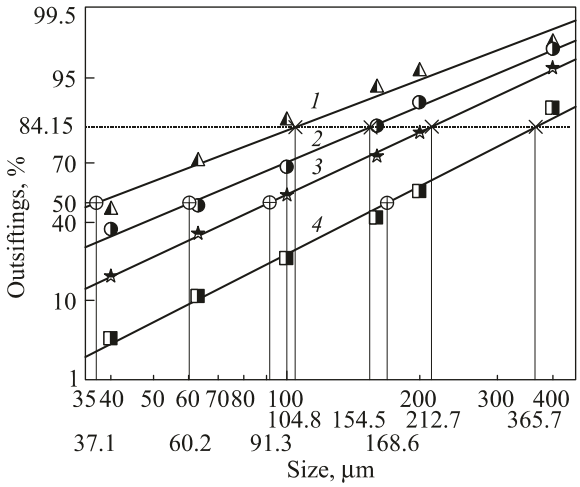

Fig. 4. Logarithmic normal size distribution of powder particles at 15 (*1*); 10 (*2*); 6.2 (*3*), and 2 MPa (*4*)

What the powders produced at different water pressures have in common is that the straight lines representing particle size distributions are inclined at similar angles (Fig. 4), i.e., the corresponding standard deviations σ are similar.

Figure 5 shows the variation of the particle size composition with the melt temperature. The dependence of the median diameter on the melt temperature t_m can approximately be described by

$$d_{50} = 44.1 + 602\{\exp(-t_m / 233) + 17.2\exp(-t_m/104)\}.$$

An increase in the melt temperature from 690 to 1000°C at 14 MPa affects the particle size composition as follows. The median diameter decreases and, thus, the powder particles become finer. This may be attributed to the increased temperature difference and heat flux and, hence, increased heat transfer coefficient, on the one hand, and improved dispersion of the melt due to lower surface tension, on the other hand.

Heat Exchange between Melt and Water. The study has revealed no developed film or nucleate boiling heat transfer in the range 650–700°C [1, 5] and no improvement of heat transfer. Therefore, the heat transfer process after the formation and during cooling of a drop can be described as follows. At first, the very high temperature difference Δt and heat flux q, which exceeds the first (q_{cr1}) and second (q_{cr2}) critical heat fluxes, cause film boiling heat transfer. The drop is enveloped by a vapor film that substantially reduces the intensity of heat transfer to the water. After q_{cr2} is exceeded, the cooling rate increases and water periodically contacts with the drop surface. The rate of decrease in temperature reaches its maximum at the final stage of cooling (nucleate boiling), i.e., after solidification of the drop.

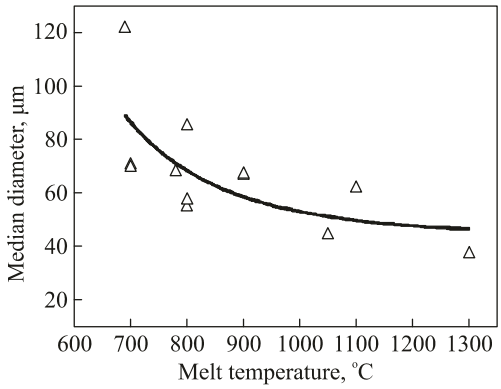

Fig. 5. Effect of the melt temperature on the particle size composition of the powder at a water pressure of 14 MPa

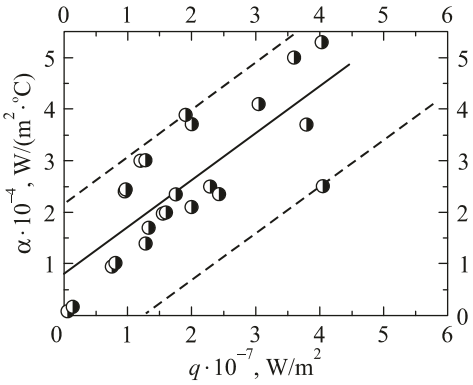

Fig. 6. Variation of the heat transfer coefficient with the heat flux at a water pressure of 10–14 MPa

Figure 6 shows the dependence of the heat transfer coefficient on the heat flux at melt temperatures 680–1000°C. An approximate formula for the average heat transfer coefficient reads as follows:

$$\alpha = 10^{-4}(0.815 + 0.9q).$$

Calculations showed that the heat transfer coefficient varies from 10^4 to $4 \cdot 10^4$ W/(m^2 · °C) as the heat flux increases from 10^7 to $5 \cdot 10^7$ W/m^2 at a water pressure of 10–15 MPa . Such a range of the heat transfer coefficient (standard deviation ± 5.5%) can be estimated small, considering the instability of heat exchange and the fact that cooled particles have different size, shape, and surface geometry.

It is characteristic that the larger the particles, the lower the heat transfer coefficient. This can be explained by the sharp reduction in heat transfer due to break of the vapor film on the irregular surface of particles.

The values of the heat transfer coefficient calculated by the empirical formulas for developed nucleate boiling [10] are by 2–3 orders of magnitude higher than the actual values. And the values calculated by the formulas for film boiling [10, 11] are by 1.5–2 orders of magnitude higher than the actual values. For example, the calculations performed in [4] using the Bromley formula cited in [11] for a drop with a diameter of 11.4 μm, t_d = = 690°C, p = 10 MPa resulted in $\alpha = 10^6$ W/(m^2 · °C). The Bromley equation is given below using the notation adopted here:

$$\alpha = 2.7\sqrt{\lambda_2 \varphi r_h \rho_2 w/\Delta t d_d}\,, \tag{10}$$

$$\varphi = 1 + c_2 \Delta t/2r_h\,, \tag{11}$$

where λ_2 is the thermal conductivity, W/(m · °C); r_h is the heat of vaporization, J/kg; ρ_2 is the density of vapor, kg/m^3; w is the speed of water jet at the time of contact with the drop, m/sec; Δt is the difference between the temperature of the melt drop t_d and the temperature of water t_w at the contact between them; c_2 is the heat capacity of vapor at the saturation temperature, J/(kg · °C). The speed w of water jet was assumed to be equal to its speed at the injector nozzle outlet, as per the formula $w = \kappa\sqrt{2gH}$, where κ is a speed coefficient, whose actual value for this particular injector is 0.85; g is the acceleration of free fall, m/sec; H is the head (height of water column), m; t_w is the saturation temperature corresponding to pressure $p = \rho w^2/2$. To calculate α, the following parameter values were used: $\lambda_2 = 5.55 \cdot 10^{-2}$ W/(m · °C); $r_h = 1.5 \cdot 10^6$ J/kg; φ = 1.736; ρ_2 = 36 kg/m^3; w = 119 m/sec; $c_2 = 5.45 \times$ $\times 10^3$ J/(kg · °C); Δt = 405°C.

Therefore, the method proposed here to determine the heat transfer coefficient by calculating the cooling rate from the dendritic parameter allows improving the reliability of calculations of heat exchange during dispersion of metal melt by high pressure water.

Determination of Parameters τ_{sph} and τ_{cool}. The time of spheroidization τ_{sph} was determined using formula (4) with a correction factor as the ratio of water density ρ_w to the vapor density ρ_v, which is more correct for film boiling.

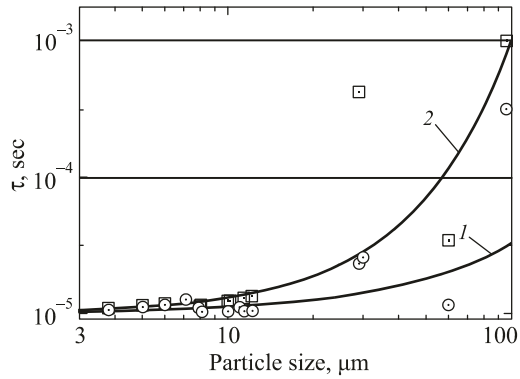

Fig. 7. Comparison of curves $\tau_{cool} = f(d_d)$ (*1*) and $\tau_{sph} = f(d_d)$ (*2*) for powders produced at a melt temperature of 690–1350°C and a water pressure of 3–15 MPa

Formula (4) with the correction factor reads as follows:

$$\tau_{sph} = \frac{3\pi^2 \mu \rho_w}{4V\gamma_m \rho_v}\left(r_{st}^4 - r_d^4\right). \quad (12)$$

The cooling time τ_{cool} for a drop was calculated from its cooling rate, determined from the experimental dendritic parameter by the procedure [8].

Figure 7 shows the variation of the spheroidizing time $\tau_{sph} = f(d_d)$ and cooling time $\tau_{cool} = f(d_d)$ with the particle size. The curves are fitted by the following formulas:

$$\tau_{sph} = 10^{(-5.4+\lg d_d)},$$

$$\tau_{cool} = 10^{(-5.26+1.23\lg 10 d_d)}.$$

Figure 7 demonstrates that the interpolation curves converge with decrease in the particle size as the spheroidization time tends to the cooling time. The curves merge when at ε = 1. This process begins when the particle size is 5–7 μm. The calculation results are confirmed by data on powder morphology (Figs. 1 and 2).

CONCLUSIONS

Water-atomized powders of aluminum and aluminum alloys, produced at a melt temperature of 690–1350°C and a water pressure of 2.0–16.0 MPa have been studied.

It has been established that the melt temperature and the water pressure (within the above ranges) very weakly affect the shape and surface geometry of particles similar in size. The particle size is a key parameter affecting the shape of particles.

Particles larger than 50 μm have an irregular shape. The larger the particles, the more there are irregularities on their surface. Particles smaller than 20–30 μm become smoother with further decrease in size. The spheroidization is complete when the particle size reaches 7–5 μm.

The heat transfer process occurs in the film boiling conditions because of high temperature differences at 380–935°C and heat flux considerably exceeding its first and second critical values. It has been established that the heat transfer coefficient at a water pressure of 10–14 MPa changes from 10^4 to $4 \cdot 10^4$ W/(m$^2 \cdot$ °C) with a standard deviation of ±5.5% with variation in the heat flux from 10^7 to $5 \cdot 10^7$ W/m^2.

This method to determine the heat transfer coefficient by calculating the cooling rate from the dendritic parameter allows improving the reliability of the calculations of heat transfer during dispersion of a melt by high-pressure water.

The size distribution of powder particles of the melt dispersed is logarithmically normal and is represented by straight lines on a logarithmic probability graphing paper, which allows determining the content of particles from two parameters: median diameter d_{50} and standard (RMS) deviation σ.

REFERENCES

1. O. S. Nichiporenko, "Shaping of powder particles during the atomization of a melt with water," *Powder Metall. Met. Ceram.*, **15**, No. 9, 665−669 (1976).
2. J. J. Dunkley, "Atomization. Powder metal technologies and applications," *ASM Int*., **7**, 35–52 (1998).
3. Lawley, Atomization, *Metal Powder Industries Federation*, Princeton, New Jersey (2003).
4. Yu. F. Ternovoi, G. A. Baglyuk, and G. S. Kudievskii, *Theoretical Basics of Spraying Metallic Melts* [in Russian], Gos. Inzh. Akad., Zaporozhe (2008), p. 298.
5. K. V. Bechke and A. F. Sanin, "Structure and properties of water-atomized aluminum powder alloy," *Powder Metall. Met. Ceram.*, **49**, No. 5–6, 266−271 (2010).
6. F. Persson, *A Study of Factors Affecting the Particle Size for Water Atomized Metal Powders*, Kungliga Tekniska Högskolan, Stockholm (2012).
7. O. D. Neikov, I. I. Odokienko, G. I. Vasil'eva, et al., "Hydrodynamic particle-size classification of aluminum alloy powders," *Powder Metall. Met. Ceram.*, **48**, No. 5–6, 249–256 (2009).
8. V. I. Dobatkin, V. I. Elagin, and V. M. Fedorov, *High-Speed Crystallized Aluminum Alloys*, Vseros. Inst. Leg. Splav., Moscow (1995), p. 335.
9. G. I. Eskin, "Non-dendritic crystallization of light alloys," *Technol. Leg. Splav.*, No. 2, 17–25 (2000).
10. O. D. Neikov, "Advanced aluminum alloy powders," in: *Handbook of Non-Ferrous Metal Powders*, Elsevier Sci. Publ. (2009), pp. 284–313.
11. N. J. Grant, "The scope and trends if developments in rapid solidification technology," in: *Proc. 5th Int. Conf. on Rapidly Quenched Metals (1984 Wurzburg, Germany),* Vol. 1, Elsevier Sci. Publ., Wurzburg (1985), pp. 3−34.
12. M. A. Mikheev and I. M. Mikheeva, *Basics of Heat Transfer* [in Russian], Energiya, Moscow (1973), p. 319.
13. S. S. Kutateladze, *Foundations of the Theory of Heat Transfer* [in Russian], Atomizdat*,* Moscow (1979), p. 383.
14. Yu. F. Ternovoi, S. S. Kudievskii, and N. R. Pashetneva, *Engineering Analysis of Molten Metal Atomization Processes* [in Russian], Gos. Inzh. Akad., Zaporozhe (2005), p. 147.
15. P. A. Kouzov, *Framework for the Analysis of Particle-Size Distribution of Industrial Dusts and Crushed Materials* [in Russian], Khimiya, Leningrad (1974), p. 280.